DOI: 10.2478/auoc-2026-0003

Ovidius University Annals of Chemistry Volume 37, Issue 1, pp. 24 - 29, 2026

Phosphate removal from aqueous solutions using slag derived from hydrogen plasma reduction of red mud

Duško KOSTIĆ*,[1] Jelena VUKOVIĆ,[1] Nebojša VASILJEVIĆ,[1] Mitar PERUŠIĆ,[1] Srećko STOPIĆ,[2] Maria Teresa BELLVER BACA,[3] Slavko SMILJANIĆ,[1] Radislav FILIPOVIĆ,[1,4] and Vladimir DAMJANOVIĆ[4]

[1]*Faculty of Technology, University of East Sarajevo, Karakaj 34 A, 75400 Zvornik, Republic of Srpska, Bosnia and Herzegovina*
[2]*IME Process Metallurgy and Metal Recycling, RWTH Aachen University, Intzestrasse 3, 52056 Aachen, Germany*
[3]*Sika Services AG, Tüffenwies 16, 8048 Zürich, Switzerland*
[4]*Nova Alumina d.o.o., Karakaj, 75400 Zvornik, Republic of Srpska, Bosnia and Herzegovina*

Abstract. In this study, the possibility of using slag derived from hydrogen-plasma reduction of red mud (H_2RMS) as a low-cost adsorbent for phosphate removal from aqueous solutions was investigated. Batch adsorption experiments were conducted to evaluate the effects of contact time, solution pH, sorbent dosage, and initial phosphate concentration under controlled laboratory conditions. Phosphate concentrations were determined spectrophotometrically using the ammonium molybdate method. These results demonstrated that phosphate adsorption onto H_2RMS is strongly pH-dependent, with maximum removal efficiency achieved under acidic conditions (pH ≈ 2). Adsorption equilibrium was achieved after approximately 18 h of contact time. Increasing the sorbent dosage enhanced phosphate removal efficiency, although improvements became marginal beyond a dosage of 10 g/L. At optimal conditions, phosphate removal efficiency of approximately 90% was achieved. These findings indicate that H_2RMS shows significant potential as an effective adsorbent for phosphate removal, offering a possible pathway for the valorization of metallurgical waste residues.

***Keywords*:** phosphate removal; red mud; hydrogen plasma reduction; red mud slag; adsorption; waste valorization.

1. Introduction

Phosphorus is a crucial element for biological systems and supports global agricultural productivity through its central role in fertilizer production. The mismanagement of phosphorus in agriculture and municipal wastewater has become a primary driver of eutrophication in freshwater and coastal ecosystems, leading to algal blooms, hypoxia, biodiversity loss, and adverse socio-economic impacts on fisheries and potable water supplies [1]. Traditional phosphorus removal technologies in wastewater treatment, such as chemical precipitation, biological nutrient removal, and membrane separation, are often obstructed by high operational cost, complex process control, and the generation of substantial sludge or chemical waste [1,2]. Adsorption has emerged as an attractive approach for phosphate removal due to its operational simplicity, adaptability to varied wastewater chemistries, and potential for material regeneration [3]. In adsorption systems, phosphate uptake mechanisms frequently involve electrostatic interactions, surface complexation, and ion exchange; adsorption efficiency is strongly influenced by material properties such as surface area, surface charge, and the presence of active metal oxyhydroxides [4–8].

Among the extensive range of adsorbent materials, industrial by-products and residues have drawn attention as cost-effective and sustainable alternatives to conventional engineered adsorbents [9, 10]. One such by-product is red mud, a highly alkaline solid residue generated during alumina production in the Bayer process. Red mud contains significant amounts of iron, aluminum, calcium, and silica oxides and its production is approximately 1-2 t per 1 t of alumina. That results in hundreds of millions of tonnes of annual global generation [11]. The large volumes and disposal challenges associated with red mud have encouraged research into its valorization for environmental remediation and resource recovery.

Red mud and its modified derivatives have been investigated for the adsorption of various aqueous contaminants, including heavy metals, arsenate, and dyes; more recently, a growing body of literature has explored its application for phosphate removal from aqueous solutions [12, 13]. Early studies on red mud as a phosphate adsorbent demonstrated that pre-treatment methods, such as acid activation or acid-thermal treatment, increase surface area and pore volume, leading to enhanced adsorption capacity compared to untreated red mud. These studies also revealed that phosphate adsorption by red mud is strongly dependent on solution pH, with higher uptake at acidic pH values, and can be described using kinetic and equilibrium models [14]. Adsorption mechanisms have been modeled through Langmuir and Freundlich isotherms,

* Corresponding author. *E-mail address:* dusko.kostic@tfzv.ues.rs.ba (Duško Kostić)

indicating both monolayer and heterogeneous surface interactions depending on the treatment and material form [15–17].

Recent work has extended red mud relevance by combining it with other materials, such as biochar, to form composite adsorbents with enhanced performance. For example, red mud-modified biochar beads demonstrated improved phosphate adsorption capacity, with mechanisms attributed to electrostatic attraction, chemical precipitation (e.g., formation of $AlPO_4$ and $FePO_4$), and physical sorption, and showed potential for phosphate recovery and slow-release fertilizer applications [14, 18]. In one of the previous researches red mud slag from carbothermal reduction was used for phosphate removal and it has showed potential for successful removal reaching 86% of removal efficiency [19].

Despite extensive research on phosphate adsorption using raw and carbothermally reduced red-mud-based materials, the potential of slag produced via hydrogen plasma reduction of red mud (H_2RMS) remains largely unexplored. Hydrogen plasma processing introduces fundamentally different physicochemical conditions compared to conventional carbothermal reduction, resulting in distinct phase composition and surface properties that may significantly influence adsorption behavior. Systematic evaluation of H_2RMS under variable operational parameters, such as contact time, solution pH, sorbent dosage, and initial phosphate concentration is essential to assess its suitability as an alternative adsorbent. Exploring this material contributes to the development of low-carbon, waste-derived adsorbents and provides new insights into the valorization potential of hydrogen-based metallurgical residues for phosphate removal.

2. Experimental

2.1. Materials and reagents

The red mud used in this study was obtained from the alumina production plant Nova Alumina Ltd. (Zvornik, Bosnia and Herzegovina).

The reagents were purchased from Semikem LTD, Vogošća, Bosnia and Herzegovina (Potassium dihydrogen phosphate, KH_2PO_4) and Sigma-Aldrich Chemie GmbH, Steinheim, Germany (hydrochloric acid HCl; sodium hydroxide pellets, NaOH; ammonium molybdate, $(NH_4)_6Mo_7O_{24}$). All chemicals used in this study were of analytical grade and were used without further purification.

2.2. Methods and equipments

2.2.1. Obtaining and characterization of the adsorbent material

The adsorbent used in this study was obtained from red mud after hydrogen plasma reduction, carried out in collaboration with the Max Planck Institute for Sustainable Materials (MPI-SusMat), Düsseldorf, Germany. Hydrogen plasma reduction of the bauxite residue was performed in an electric arc furnace (EAF, custom-designed experimental setup) designed for high-temperature plasma processing. In this system, the charge material is exposed directly to the electric arc generated between graphite electrodes, enabling rapid heating and reduction reactions at temperatures approaching 1800 °C [19, 20].

During the process, the furnace chamber was operated under a controlled atmosphere consisting of argon with approximately 10 % hydrogen. Under these conditions, iron oxides present in red mud are reduced to metallic iron, which separates from the remaining oxide melt. The process results in the formation of two phases: a metallic iron fraction and a slag phase enriched with oxides of aluminum, titanium, silicon, and calcium. The slag phase obtained after separation was used as the adsorbent material in the present work.

The mineralogical composition of the H_2RMS adsorbent was analyzed using X-ray diffraction (XRD) with a Bruker D8 Advance diffractometer (Bruker AXS GmbH, Karlsruhe, Germany). Phase identification was performed using Diffrac.EVA software (Bruker AXS, Germany) by comparing the obtained diffraction patterns with the reference database.

The elemental composition of the adsorbent material was determined using X-ray fluorescence spectroscopy (XRF) with an AMETEK spectrometer (AMETEK Inc., Pennsylvania, USA).

2.2.2. Determination of phosphate

Phosphate concentrations in aqueous samples were determined using the molybdenum blue spectrophotometric method, in which phosphate ions react with ammonium molybdate under acidic conditions to form a phosphomolybdate complex that is subsequently reduced to a blue-colored compound measurable by UV–Vis spectrophotometry at 880 nm. The absorbance of the developed color is proportional to the phosphate concentration in solution.

All calibration standards and sample measurements were prepared and analyzed in accordance with the Water quality—Determination of phosphorus—Spectrometric method using ammonium molybdate (BAS ISO 6878:2004) standard [22].

For each sample, absorbance measurements were performed in triplicate using the UV–Vis spectrophotometer. The reported phosphate concentrations represent the average of three successive measurements, and the corresponding standard deviation was calculated to assess the analytical repeatability of the method.

2.2.3. Batch adsorption experiments

Phosphate adsorption experiments were carried out under batch conditions at room temperature. The effects of contact time, solution pH, sorbent dosage, and initial phosphate concentration on adsorption performance were systematically investigated.

A known mass of H_2RMS adsorbent was added to Falcon tubes containing phosphate solution of a defined initial concentration. The tubes were placed horizontally on a laboratory shaker and mixed at a constant speed of 120 rpm to ensure homogeneous mixing. The pH of the solution was adjusted to the desired value prior to the adsorption experiments using appropriate acidic or alkaline solutions.

After the predetermined contact time elapsed, the solid and liquid phases were separated using a

laboratory centrifuge. The supernatant was carefully decanted and further filtered through qualitative filter paper (blue ribbon) to remove any remaining suspended particles. The residual phosphate concentration in the filtrate was measured using a UV–Vis spectrophotometer (Shimadzu UV-1800, Japan).

2.2.4. Evaluation of adsorption performance

The adsorption performance of H_2RMS was evaluated in terms of phosphate removal efficiency and adsorption capacity.

The adsorption capacity at equilibrium, q_e (mg/g) was calculated using the mass balance equation:

$$q_e = \frac{(C_0 - C_e)V}{m} \quad (1)$$

The phosphate removal efficiency (R, %) was calculated as:

$$R = \frac{(C_0 - C_e)}{C_0} 100 \quad (2)$$

where C_0 (mg/L) is the initial phosphate concentration, C_e (mg/L) is the equilibrium phosphate concentration, V (L) is the volume of the solution, and m (g) is the mass of the adsorbent.

3. Results and discussion

3.1. Characterization of the adsorbent material

The chemical composition of the H_2RMS slag determined by XRF analysis is presented in Table 1.

Table 1. Chemical composition of hydrogen-plasma-reduced red mud slag (H_2RMS) [21]

Compounds	Content (mass %)
FeO	20.2%
Al_2O_3	17%
SiO_2	14%
TiO_2	10.2%

The H_2RMS is primarily composed of iron oxide (FeO), alumina (Al_2O_3), silica (SiO_2), and titanium dioxide (TiO_2), which together constitute the dominant oxide phases of the material. The high content of iron- and aluminum-based oxides is particularly relevant for phosphate adsorption, as these phases are known to provide active surface sites for phosphate binding under acidic conditions.

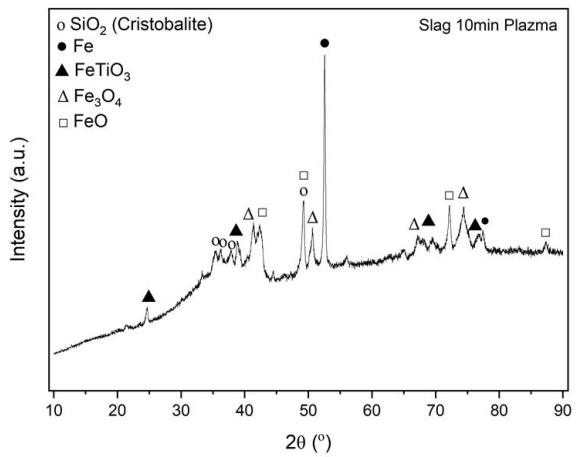

Figure 1. XRD analysis of H_2RMS [21]

Phase composition of the H_2RMS was analyzed by X-ray diffraction (XRD). The XRD patterns confirmed the complete reduction of hematite originally present in red mud. Hematite was transformed into magnetite, wüstite, and/or metallic iron, indicating the high efficiency of iron reduction during the plasma-thermal process.

In addition, ilmenite presence ($FeTiO_3$) was detected, suggesting that titanium remained chemically stable during hydrogen plasma treatment and did not participate in the reduction reactions. The XRD analysis identified silicon oxide (cristobalite) as the dominant crystalline phase. Aluminum- and calcium-containing phases, although confirmed by ICP analysis, were not detected by XRD, indicating that these elements were predominantly present in amorphous phases that cannot be seen by X-ray diffraction.

3.2. Effect of the contact time

The effect of the contact time on phosphate adsorption by H_2RMS was investigated over a time range of 1 to 24 h (1, 3, 6, 9, 12, 18, and 24 h). These experiments were conducted using a sorbent dosage of 5 g/L, an initial phosphate concentration of 14.34 mg/L, and a solution pH of 2.21. The acidic pH was intentionally selected based on previous findings indicating that red mud and red-mud-derived slags exhibit improved phosphate uptake under strongly acidic conditions.

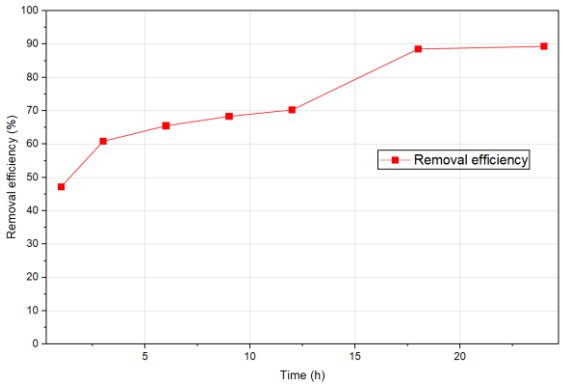

Figure 2. Effect of contact time on process efficiency (14.34 mg/L, pH = 2.21)

As shown in Figure 2, phosphate removal increased progressively with contact time, indicating continuous occupation of available adsorption sites on the H_2RMS surface. A rapid increase in removal efficiency was observed during the initial hours of contact, which can be attributed to the abundance of active surface sites and a high concentration gradient between the solution and the adsorbent surface. With increasing contact time, the rate of phosphate uptake gradually decreased, suggesting partial saturation of adsorption sites.

Adsorption equilibrium was reached after approximately 18 h (1080 min), at which a removal efficiency of 88.5% was achieved. Further prolongation of the contact time to 24 h resulted in only a marginal increase in removal efficiency, indicating that equilibrium conditions had already been established. This behavior is characteristic of adsorption processes governed by surface complexation and diffusion-controlled mass transfer, where the adsorption rate

decreases as surface sites become progressively occupied.

3.3. Effect of solution pH

After establishing the optimal contact time of 18 h, the influence of solution pH on phosphate adsorption was examined over a wide pH range (approximately pH 1 to pH 12). The results are presented in Figure 3.

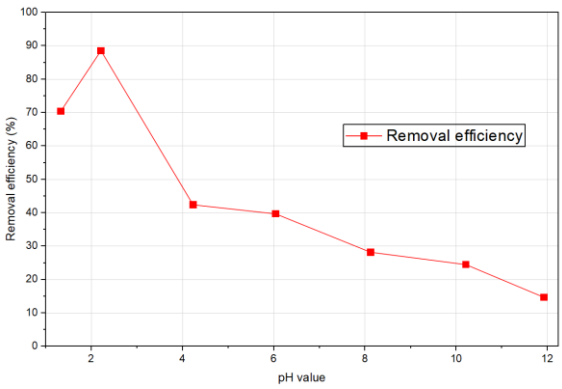

Figure 3. Effect of solution pH on process efficiency

The adsorption efficiency of phosphate onto H_2RMS exhibited a strong dependence on solution pH. The highest removal efficiency was observed under acidic conditions, with a maximum at pH ≈ 2. As the pH increased beyond this value, a pronounced decline in adsorption efficiency was recorded.

This behavior can be explained by changes in both phosphate species present and the surface charge of the adsorbent. Under acidic conditions, the H_2RMS surface is likely protonated, promoting electrostatic attraction between positively charged surface hydroxyl groups and negatively charged phosphate species (primarily dihydrogen phosphate, $H_2PO_4^-$). In addition, iron- and aluminum-containing phases present in the slag can form inner-sphere surface complexes with phosphate ions, further enhancing adsorption at low pH [6].

At higher pH values, increased competition with hydroxyl ions and progressive deprotonation of surface functional groups reduce electrostatic attraction and inhibit phosphate binding. The observed pH dependence is consistent with adsorption mechanisms reported for iron- and aluminum-rich adsorbents derived from red mud and other metallurgical residues [23–25].

3.4. Effect of sorbent dosage

The effect of sorbent dosage on phosphate adsorption was investigated using four different H_2RMS dosages: 1, 5, 10, and 20 g/L All experiments were conducted at a contact time of 18 h and pH ≈ 2. The results are shown in Figure 4.

An increase in sorbent dosage resulted in a corresponding increase in phosphate removal efficiency, reflecting the greater availability of adsorption sites with increasing amounts of adsorbent. At a dosage of 1 g/L, removal efficiency was relatively low, while a substantial improvement was observed at 5 g/L.

However, further increasing the dosage beyond 10 g/L led to only minor improvements in removal efficiency. At dosages of 10 and 20 g/L, phosphate removal efficiencies of 94.3% and 96.3%, respectively, were achieved. This behavior suggests that, beyond a certain adsorbent concentration, the system becomes limited by the available phosphate ions rather than by the number of active adsorption sites.

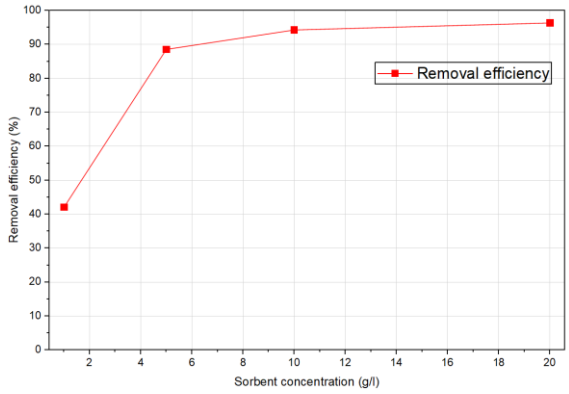

Figure 4. Effect of sorbent dosage on process efficiency

From a practical perspective, these results indicate that increasing the sorbent dosage above 10 g/L does not provide a significant benefit and may be economically inefficient for large-scale applications.

3.5. Effect of initial phosphate concentration

The influence of initial phosphate concentration on adsorption performance was evaluated by comparing solutions with different concentrations relative to the base concentration of 14.43 mg/L. A five-fold higher concentration (71.7 mg/L), a five-fold lower concentration (2.86 mg/L), and a ten-fold lower concentration (1.43 mg/L) were tested. All experiments were performed using a sorbent dosage of 5 g/L, pH ≈ 2, and a shaking speed of 120 rpm at room temperature.

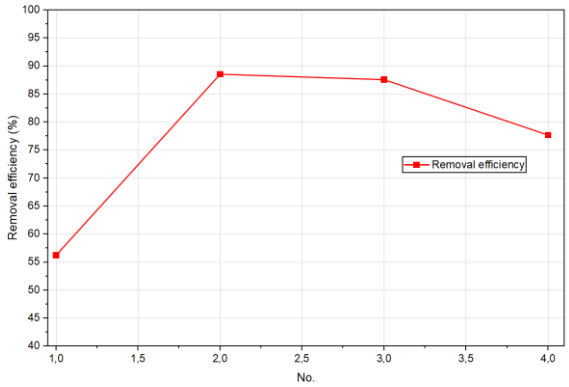

Figure 5. Effect of initial phosphate concentration on process efficiency

As illustrated in Figure 5, the highest removal efficiency (88.55%) was obtained at the initial phosphate concentration of 14.43 mg/L A very similar removal efficiency (87.59%) was observed at the five-fold lower concentration, indicating that H_2RMS is effective for phosphate removal at low to moderate phosphate levels.

At the highest initial concentration (71.7 mg/L), the removal efficiency decreased, which can be attributed to saturation of available adsorption sites and insufficient sorbent capacity relative to the phosphate load. These results suggest that H_2RMS is particularly suitable for phosphate removal from wastewaters with low to moderate phosphate concentrations, such as municipal effluents or secondary treatment streams.

4. Conclusions

This study demonstrated the potential of slag derived from hydrogen plasma reduction of red mud (H_2RMS) as an effective adsorbent for phosphate removal from aqueous solutions. Batch adsorption experiments showed that phosphate adsorption potential by H_2RMS is strongly influenced by contact time, pH of the solution, sorbent dosage, and initial phosphate concentration. Adsorption equilibrium was achieved after approximately 18 h, indicating relatively rapid achievement of equilibrium conditions.

The adsorption process exhibited strong pH dependence, with maximum phosphate removal observed under strongly acidic conditions (pH ≈ 2). This behavior can be attributed to favorable electrostatic interactions and surface complexation between phosphate species and iron- and aluminum-containing phases present in the slag. Increasing the sorbent dosage enhanced phosphate removal efficiency; however, improvements became less significant beyond a dosage of 10 g/L. The adsorbent demonstrated high removal efficiencies for low to moderate initial phosphate concentrations, with approximately 90% removal achieved at initial concentrations of 2.9-14.4 mg/L.

Overall, the results indicate that H_2RMS represents a promising low-cost adsorbent for phosphate removal, offering a viable pathway for the valorization of metallurgical waste residues. Future work should focus on adsorption capacity modeling, investigation of the possibility for regeneration and reuse of the adsorbent, and evaluation of performance in real wastewater systems to further assess the practical applicability of this material.

Conflict of interest

The authors declare that there is no conflict of interest concerning the publication of this research article.

Acknowledgements

This research was funded by the European Commission, grant number 101135077 (EURO-TITAN).

References

[1]. M.N. Nadagouda, G. Varshney, V. Varshney, C.A. Hejase, Recent advances in technologies for phosphate removal and recovery: A Review, ACS Environmental Au 4 (2024) 271–291. https://doi.org/10.1021/ACSENVIRONAU.3C00069

[2]. W.S. Chai, J.Y. Cheun, P.S. Kumar, M. Mubashir, Z. Majeed, F. Banat, S.H. Ho, P.L. Show, A review on conventional and novel materials towards heavy metal adsorption in wastewater treatment application, Journal of Cleaner Production 296 (2021) 126589. https://doi.org/10.1016/J.JCLEPRO.2021.126589

[3]. A. Gizaw, F. Zewge, A. Kumar, A. Mekonnen, M. Tesfaye, A comprehensive review on nitrate and phosphate removal and recovery from aqueous solutions by adsorption, AQUA - Water Infrastructure, Ecosystems and Society 70 (2021) 921–947. https://doi.org/10.2166/AQUA.2021.146

[4]. S. Kumari, Y. Dong, S.I. Safferman, Phosphorus adsorption and recovery from waste streams using biochar: review of mechanisms, modifications, and agricultural applications, Applied Water Science 15 (2025) 162. https://doi.org/10.1007/S13201-025-02523-0

[5]. P. Loganathan, S. Vigneswaran, J. Kandasamy, N.S. Bolan, Removal and recovery of phosphate from water using sorption, Crit. Rev. Environ. Sci. Technol. 44 (2014) 847–907. https://doi.org/10.1080/10643389.2012.741311

[6]. A. Bhatnagar, E. Kumar, M. Sillanpää, Fluoride removal from water by adsorption—A review, Chemical Engineering Journal 171 (2011) 811–840. https://doi.org/10.1016/j.cej.2011.05.028

[7]. S. Babel, T.A. Kurniawan, Low-cost adsorbents for heavy metals uptake from contaminated water: a review, Journal of Hazardous Materials 97 (2003) 219–243. https://doi.org/10.1016/S0304-3894(02)00263-7

[8]. Y.S. Ho, G. McKay, Sorption of dye from aqueous solution by peat, Chemical Engineering Journal 70 (1998) 115–124. https://doi.org/10.1016/s0923-0467(98)00076-1

[9]. A. Bhatnagar, M. Sillanpää, Utilization of agro-industrial and municipal waste materials as potential adsorbents for water treatment—A review, Chemical Engineering Journal 157 (2010) 277–296. https://doi.org/10.1016/j.cej.2010.01.007

[10]. M. Ahmaruzzaman, Industrial wastes as low-cost potential adsorbents for the treatment of wastewater laden with heavy metals, Advances in Colloid and Interface Science 166 (2011) 36–59. https://doi.org/10.1016/j.cis.2011.04.005

[11]. Y. Wang, L. Li, Z. Liu, Z. Ren, Frontier research and prospect of phosphate adsorption in wastewater by red mud: a review, Desalination and Water Treatment 310 (2023) 86–108. https://doi.org/10.5004/DWT.2023.29958

[12]. W. Huang, S. Wang, Z. Zhu, L. Li, X. Yao, V. Rudolph, F. Haghseresht, Phosphate removal from wastewater using red mud, Journal of Hazardous Materials 158 (2008) 35–42. https://doi.org/10.1016/J.JHAZMAT.2008.01.061

[13]. Y. Zhao, Q. Yue, Q. Li, X. Xu, Z. Yang, X. Wang, B. Gao, H. Yu, Characterization of red mud granular adsorbent (RMGA) and its performance on phosphate removal from aqueous solution, Chemical Engineering Journal 193–194 (2012) 161–168. https://doi.org/10.1016/J.CEJ.2012.04.040

[14]. F. Tian, Y. Wang, M. Qi, R. Sun, Y. Zhao, L. Wang, S. Wu, Phosphate Recovery from Wastewater Using Red Mud-Modified Biochar Beads: Performance and Mechanism Study, Water 17 (2025) 2699. https://doi.org/10.3390/W17182699

[15]. I. Langmuir, The adsorption of gases on plane surfaces of glass, mica and platinum, Journal of the

American Chemical Society 40 (1918) 1361–1403. https://doi.org/10.1021/ja02242a004
[16]. K.Y. Foo, B.H. Hameed, Insights into the modeling of adsorption isotherm systems, Chemical Engineering Journal 156 (2010) 2–10. https://doi.org/10.1016/j.cej.2009.09.013
[17]. H. Freundlich, Über die Adsorption in Lösungen, Zeitschrift Für Physikalische Chemie 57U (1907) 385–470. https://doi.org/10.1515/zpch-1907-5723
[18]. J. Ye, X. Cong, P. Zhang, E. Hoffmann, G. Zeng, Y. Liu, W. Fang, Y. Wu, H. Zhang, Interaction between phosphate and acid-activated neutralized red mud during adsorption process, Applied Surface Science 356 (2015) 128–134. https://doi.org/10.1016/J.APSUSC.2015.08.053
[19]. J. Vuković, S.N. Smiljanić, D. Kostić, S. Stopić, M. Perušić, N. Vasiljević, A preliminary assessment of the use of red mud slag for phosphate sorption from aqueous solutions, Engineering Proceedings 99 (2025) 5. https://doi.org/10.3390/ENGPROC2025099005
[20]. S. Stopic, R. Schneider, D. Kostic, I.R. Souza Filho, M. Perušic, E. Emil-Kaya, B. Friedrich, Combined decarbonizing technologies for treatment of bauxite residues, Waste 3 (2025) 11. https://doi.org/10.3390/WASTE3020011
[21]. D. Kostić, Innovative Approaches to the Production of Titanium(IV) Oxide Nanopowders from Secondary Raw Materials, University of East Sarajevo, Faculty of Technology, 2025.
[22]. ISO 6878:2004 - Water quality — Determination of phosphorus — Ammonium molybdate spectrometric method, (n.d.). https://www.iso.org/standard/36917.html (Last accessed March 8, 2026).
[23]. L. Zhang, Y. Gao, Y. Xu, J. Liu, Different performances and mechanisms of phosphate adsorption onto metal oxides and metal hydroxides: A comparative study, Journal of Chemical Technology and Biotechnology 91 (2016) 1232–1239. https://doi.org/10.1002/jctb.4710.
[24]. Y. Kim, R.J. Kirkpatrick, An investigation of phosphate adsorbed on aluminium oxyhydroxide and oxide phases by nuclear magnetic resonance, European Journal of Soil Science 55 (2004) 243–251. https://doi.org/10.1046/j.1365-2389.2004.00595.x
[25]. X. Wang, B.L. Phillips, J.F. Boily, Y. Hu, Z. Hu, P. Yang, X. Feng, W. Xu, M. Zhu, Phosphate sorption speciation and precipitation mechanisms on amorphous aluminum hydroxide, Soil Systems 3 (2019) 20. https://doi.org/10.3390/soilsystems3010020

Received: 20.02.2026
Received in revised form: 19.03.2026
Accepted: 21.03.2026